Preprints, *Sixth Conference on Mesoscale Processes*, July 1994, Portland, Oregon

P3.1 JET-INDUCED INERTIAL INSTABILITIES AND MESOSCALE CONVECTIVE SYSTEM GROWTH

David O. Blanchard
NOAA/National Severe Storms Laboratory
Boulder, Colorado

William R. Cotton
Dept. of Atmospheric Science
Colorado State University
Fort Collins, Colorado

1. INTRODUCTION

Many mesoscale convective complexes (MCCs) and mesoscale convective systems (MCSs) have been observed to form in environments where the isentropic absolute vorticity may have values that approach zero, resulting in regions with weak inertial stability. Further, if certain vertical stability criteria are met, then symmetric instability may also be present. It has been demonstrated that for a given amount of convective available potential energy (CAPE), deep convective circulations can be modified and enhanced as the symmetric stability is reduced (Emanuel 1982; Xu 1986). Consequently, there has been speculation that the evolution and organization of convection into MCCs (Maddox 1983) and MCSs may be related to the presence of an environment in which the inertial stability is weak or unstable (Emanuel 1979, 1982, 1983; Jascourt et al. 1988; Blanchard 1992). Two typical regions in which these environmental conditions are met are 1) just equatorward of a wind maximum where the anticyclonic shear is large, and 2) in subsynoptic-scale ridges where the anticyclonic curvature is large.

In some mesoscale environments, particularly in the springtime over the continental U.S. when CAPE is large and a strong jet stream is still present, the atmosphere is unstable to both upright and slantwise convection. The latter is often referred to as conditional symmetric instability (CSI). Because the time scales of upright and slantwise convection are considerably different, upright convection will typically dominate. It is hypothesized that this upright convection can, over longer time scales, exploit the weak restoring force present in the mesoscale inertial stability. Air parcels move vertically through upright convection and on reaching the equilibrium level expand preferentially in the region that is inertially least stable. Recent modeling work by Seman (1992) suggests that parcel descent occurs on slant trajectories taking the path of least resistance, is directed back toward the generating convection, and occurs preferentially in the inertially unstable region.

In recent papers (Raymond and Jiang 1990; Raymond 1992; Seman 1990, 1992;), the concept of in situ generation of potential vorticity anomalies was developed to explain the upscale growth of convection into mature mesoscale systems. In these studies, there were no regions of inertial instability (i.e., negative potential vorticity) before the onset of convection; the convection itself was responsible for the development of the inertial instability. Although these models are very appealing because they can generate many of the features found in MCCs and MCSs, they fail to address the question of why only some, instead of all, convective systems achieve this condition and grow upscale. A likely explanation may be found in this work.

If the environment is already predisposed to a state of weak inertial stability, as suggested by the typical environments in which MCSs occur, then the divergent outflow at the equilibrium level can exploit the weak restoring force in the inertially unstable (or weakly stable) region. The consequence would be an increase of the upper tropospheric divergence of the cloud and would result in continued stronger updrafts, lower-level perturbation pressure falls and, eventually, the slant downdrafts suggested by CSI theory. Further, the convection is required to do less work to achieve the final state of an upper-level (low-level) negative (positive) potential vorticity anomaly.

To explore the hypothesis that inertial instability plays a role in the development of mesoscale organization of convection, MCSs that occurred in the data-rich PRE-STORM network, and MCS environments sampled with new technology were previously examined (Blanchard 1992). To continue to investigate the role of inertial stability, we used a mesoscale model to simulate these environments using idealized conditions. The model simulations were executed as a series of sensitivity tests with different degrees of inertial [in]stability to develop a comprehensive understanding of the dynamics of this type of atmospheric motion. Results from these numerical simulations are discussed below and are compared with observations.

2. MODEL DESCRIPTION

The model used in this study is the Regional Atmospheric Modeling System (RAMS), developed at Colorado State University. RAMS is a nonhydrostatic, primitive equation model and has been discussed extensively in the literature, most recently by Pielke et al. (1992).

The model simulations used a two-dimensional domain of 200 horizontal points in the *x*-direction with 5 km spacing, and 40 vertical points with 600 m spacing. A nonhydrostatic rigid wall on top was selected for the upper boundary condition. A Rayleigh friction absorbing layer was used in the top six levels to prevent reflection of upwardly propagating gravity waves. Lateral boundaries used the Klemp-Wilhelmson condition.

The base state environment in the model simulation has no jet in the wind field. Instead, the jet was imposed as a perturbation on the base state winds and allowed to grow for 72 h using a function of the form

$$F_v = V_0 e^{-\alpha^2 (x-x_0)^2} e^{-\beta^2 (z-z_0)^2} \tag{1}$$

where V_0 [m s^{-1}] is the amplitude of the jet forcing, and α and β are horizontal and vertical wavenumbers. After 72 h, the simulation was suspended and used as the starting condition for subsequent simulations.

The convective heating was explicitly imposed using a function of the form

$$F_H = H_0 e^{-\alpha^2 (x-x_0)^2} e^{-\beta^2 (z-z_0)^2} \tag{2}$$

where H_0 [°C h^{-1}] is the amplitude of the forced heating, and α and β are horizontal and vertical wavenumbers.

Note that while the simulations occur in the (x,z) plane, the wind shear i the meridional direction, perpendicular to this plane such that the ambient zonal wind is parallel to the axes of the circulations that develop. This is different from many two-dimensional simulations in which the wind blows in the plane of the simulations. The geometry is set up this way so that the combined dynamical effects of baroclinic shear and Coriolis rotation can be studied. This geometry is essentially the same as that employed by Seman (1990) in his study of Conv-SI (convective-symmetric instability)

We note that the wind can be decomposed into a velocity potential (irrotational), φ, and a stream function (non-divergent), ψ. Then, the Cartesian coordinates of the wind can be written as

$$u = -\frac{\partial \psi}{\partial y} - \frac{\partial \phi}{\partial x}; \qquad v = -\frac{\partial \psi}{\partial x} - \frac{\partial \phi}{\partial y}, \tag{3}$$

and the vorticity and divergence can be expressed as

$$\begin{aligned} \nabla^2 \psi &= \zeta_z \equiv \left(\partial v/\partial x - \partial u/\partial y \right) \\ \nabla^2 \phi &= -\delta \equiv -\left(\partial u/\partial x + \partial v/\partial y \right) \end{aligned} . \tag{4}$$

If we restrict ourselves to working in the *x*-*z* domain we can rewrite (4) as

$$\begin{aligned} \nabla^2 \psi &= \zeta_z \equiv \partial v/\partial x \\ \nabla^2 \phi &= -\delta \equiv -\partial u/\partial x \end{aligned} . \tag{5}$$

As can be clearly seen, the rotational component of the wind is completely described by the *v*-component, and the divergence is completely described by the *u*-component of the wind. Because we are investigating the possibility that inertial instability can increase the cross-stream flow, and we have designed our experiment so that the jet flow is into the page, the only component of divergence that should be modified by changes in the inertial stability is in the east-west direction.

3. RESULTS

Twenty-four experiments were run using three heating rates (1, 3, and 5 °C h^{-1}), four jet speeds (0, 10, 20, and 30 m s^{-1}), and two latitudes (25° and 40°).

Control experiments were conducted with no jet imposed on the base state using all three heating rates and both latitudes. After the heating function was allowed to interact with the environment, upper-level outflow developed above the level of maximum heating and below the tropopause. The outflow was symmetric about the domain; e.g., the outflow had equal strength in both directions (not shown). The results of these experiments indicate that the strength of the outflow increased with the stronger heating rates (stronger updraft), and decreased at the higher latitude (increasing inertial stability). These are, of course, what we should expect.

The next simulation has a jet imposed on the base state winds. The forcing functions (1) and (2) were set

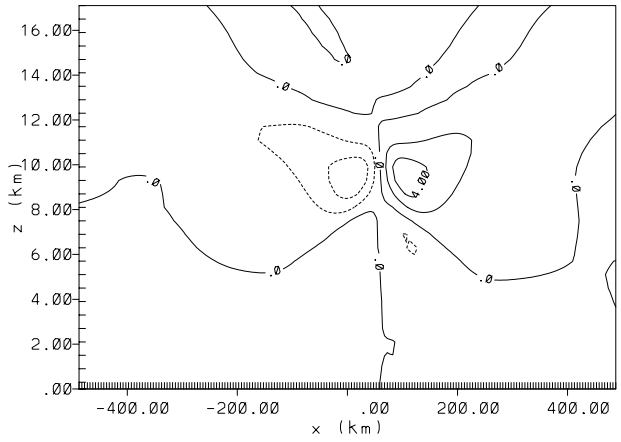

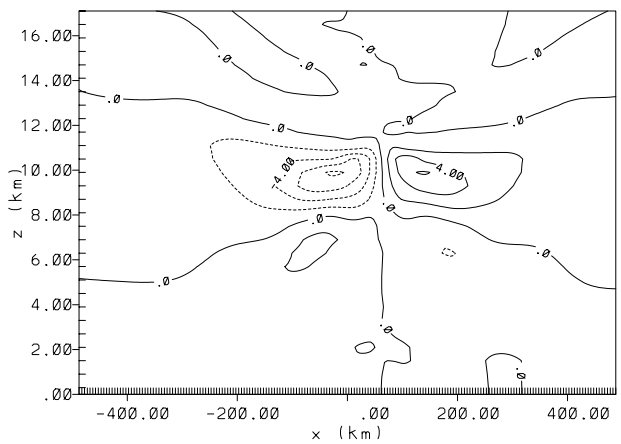

Figure 1. X-Z cross section showing the u-component of the wind. Heating function is centered near +50 km and 8 km. Contours every 0.5 m s^{-1}; negative values are dashed. (a) after 3 h; (b) after 6 h.

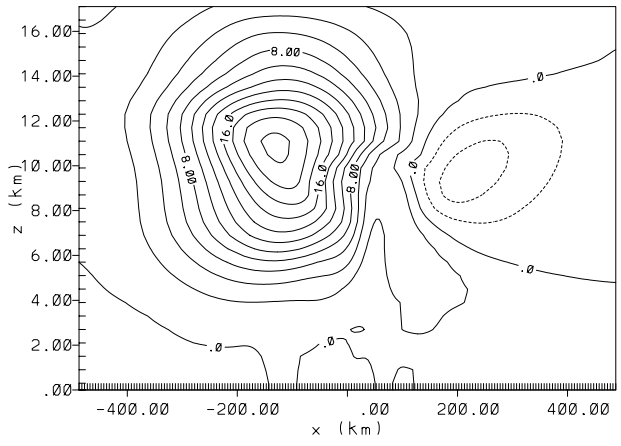

Figure 2. X-Z cross section showing the v-component of the wind after 6 h simulation time. Contours every 2 m s^{-1}; negative values are dashed

to impose a jet of 30 m s^{-1}, and a heating rate of 3°C h^{-1}. Asymmetric outflow develops after only a few hours

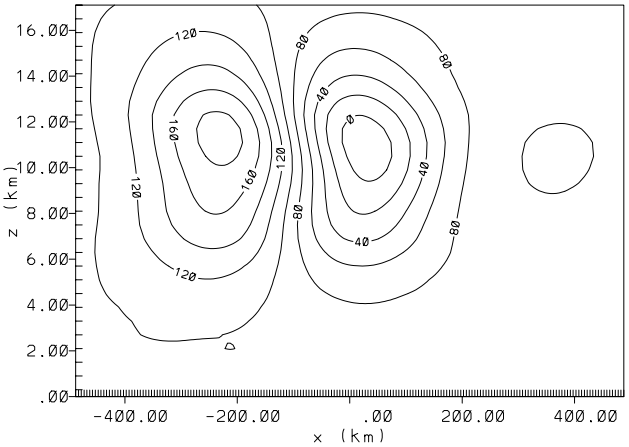

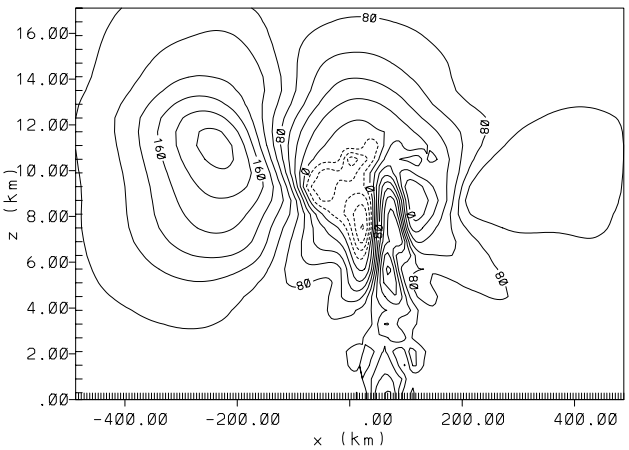

Figure 3. X-Z cross section showing the evolution of the absolute vorticity field at (a) 0 h, and (b) 6 h. Contours every 20x10^{-6} s^{-1}; negative values are dashed.

(Fig. 1a). The outflow towards the left (west) is stronger than its counterpart to the right (east). By 6 h (Fig 1b), the easterly winds are in excess of -8.0 m s^{-1}, whereas the westerly winds are weaker and approach +6.0 m s^{-1}. The rotational component of the flow (v) has also been perturbed and has strengthened the jet on the left side of the heating and weakened it on the right side (Fig 2). Further, the evolution of the u-component of the wind has tended to advect lower momentum air to the west and to tighten the gradient of the jet. This results in additional inertial destabilization. Starting with a vorticity couplet (Fig. 3a) with values only slightly less than zero initially, we now have a region that is very negative (Fig. 3b), and consequently, inertially unstable. This inertially unstable region is the result of local vorticity generation superimposed on a larger-scale background that was near neutral in stability.

It is instructive to compare the results of a whole class of experiments to assess what is occurring in the regions of weak stability. Figure 4 reveals the time rate

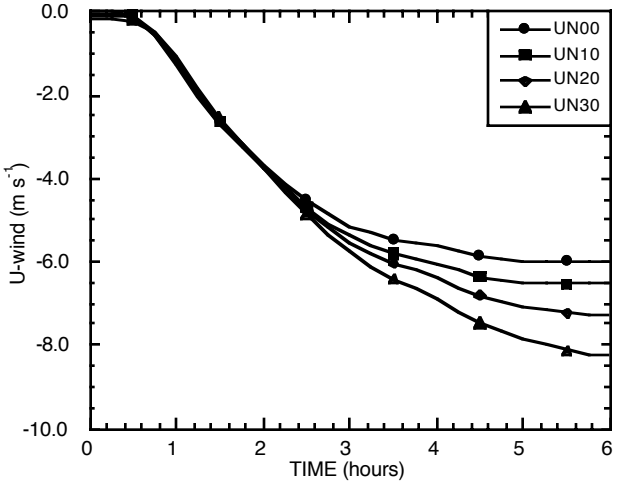

Figure 4. Evolution of the divergent u-winds as a funtion of time. The four jet simulations (0, 10, 20, and 30 m s^{-1}) are labled as UN00, UN10, UN20, and UN30, respectively. Wind speeds are m s^{-1}; heating rate is 3 °C h^{-1}.

of change of the point value maximum of the easterly component of diverging outflow. Results from four different jet core strengths (0, 10, 20, and 30 m s^{-1}) are shown. Clearly, after about two hours of simulation the easterly outflow is larger for stronger jets. The westerly component (not shown) showed no similar structure; the point value maximum increased slightly with time, but did not vary with increasing jet speeds. In the inertially unstable region, the efficient evacuation of diverging cloud mass permits stronger updrafts (not shown) to develop over time. These updrafts, in turn, advect additional low-level, low-momentum air to upper levels where it increases the horizontal gradient of the wind (and, hence, the inertial instability) near the jet, resulting in a positive feedback process similar to that described by Eliassen (1951).

Regions of isentropic inertial instability are typically short-lived and small in scale. To adequately sample these regions, large numbers of observations with high spatial and temporal resolution are required. Figure 5 shows an example of high resolution data capturing a mesoscale region of inertial instability. Convection began during the afternoon in southwest Oklahoma and produced numerous severe thunderstorms; subsequent storms formed in central and northeast Oklahoma. These storms were not as severe and eventually evolved into a MCC in the region of inertial instability. Convection that was not located in this dynamically unstable region quickly dissipated after dark, supporting the hypothesis that the mesoscale instability had an important role in sustaining the convection long enough to permit an upscale growth through geostrophic adjustment processes.

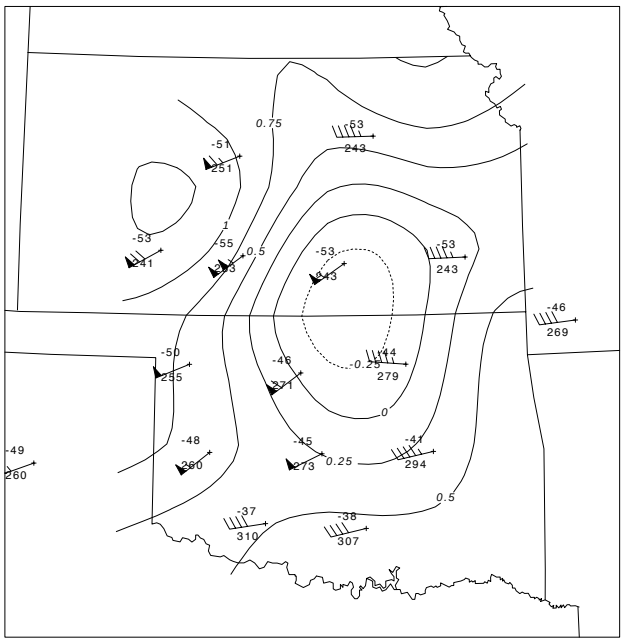

Figure 5. Plot of isentropic inertial instability, defined as $(\zeta+f)/f$, for 13 May 1985 at 0000 UTC on the 330 K isentrope. Contours every 0.25; negative values are dashed. Station plots show temperature (°C) in the upper left and the pressure (mb) in the lower left.

4. REFERENCES

Blanchard, D.O., 1992. Evolution of a mesoscale convective complex: The role of inertial instability. *Preprints, 5th Conference on Mesoscale Processes.* American Meteorological Society, Boston, Mass., 341–346.

Eliassen, A., 1951. Slow thermally or frictionally controlled meridional circulations in a circular vortex. *Astrophys. Norv.*, **5**: 19–60.

Emanuel, K.A., 1979. Inertial instability and mesoscale convective systems. Part I: Linear theory of inertial instability in rotating viscous fluids. *J. Atmos. Sci.*, **36**: 2425–2449.

————, 1982. Inertial instability and mesoscale convective systems. Part II: Symmetric CISK in a baroclinic flow. *J. Atmos. Sci.*, **39**: 1080–1097.

———— , 1983. The Lagrangian dynamics of moist symmetric instability. *J. Atmos. Sci.*, **40**: 2368–2376.

Jascourt, S.D., S.S. Lindstrom, C.J. Seman, and D.D. Houghton, 1988. An observation of banded convective development in the presence of weak symmetric stability. *Mon. Wea. Rev.*, **116**: 175–191.

Maddox, R.A., 1983. Large–scale meteorological conditions

associated with mid-latitude convective complexes. *Mon. Wea. Rev.*, **111**: 1475–1493.

Pielke, R.A., W.R. Cotton, R.L. Walko, C.J. Tremback, W.A. Lyons, M.E. Nicholls, M.D. Moran, D.A. Wesley, T.J. Lee, and J.H. Copeland, 1992. A comprehensive meteorological modeling system — RAMS. *Meteorol. Atmos. Phys.*, **49**: 69–91.

Raymond, D.J., 1992. On the formation of jets and vortices in mesoscale convective systems. Preprints, *5th Conference on Mesoscale Processes*. American Meteorological Society, Boston, Mass., 333–336.

————— and H. Jiang, 1990. A theory for long-lived mesoscale convective systems. J. Atmos. Sci., 47: 3067–3077.

Seman, C.J. 1990. Numerical simulation of deep moist convection in a baroclinic atmosphere. Preprints, 4th Conference on Mesoscale Processes, American Meteorological Society, Boston, Mass., 104–105.

————— , 1992. On the role of nonlinear convective-symmetric instability in the evolution of a numerically simulated mesoscale convective system. Preprints, 5th Conference on Mesoscale Processes. American Meteorological Society, Boston, Mass., 282–287.

Xu, Q., 1986. Conditional symmetric instability and mesoscale rainbands. *Quart. J. R. Met. Soc.*, **112**: 315–334.